International Journal of Mechanical Engineering Research (IJMER)
Volume 4, Issue 1,Pages 6-10, March 2016,ISSN: 2347-47XX

Prediction of temperature distribution and weld pool geometry for 304 stainless steel using TIG welding parameters

Mohd Anees Siddiqui[1], K.M.Moeed[2], S.A.H. Jafri[3]
[1,2]University Polytechnic, Integral University Lucknow, INDIA
[3] Department of Mechanical Engineering, Integral University Lucknow, INDIA
[1]anees@iul.ac.in, [2]moeed@iul.ac.in, [3]sahjafri@iul.ac.in

Abstract—A steady state conduction model of fusion was developed by using SmartWeld simulation application in order to predict the temperature distribution and the effect of process parameters on weld pool during the TIG welding operation of 304 stainless steel. The planning of simulation runs has been performed in accordance with the Taguchi L9 design with two factors, each three levels. The process parameters considered are weld speed and input power during TIG welding. Multiple linear regression analysis is performed in order to analyze the effect of process parameters on length, width and depth of weld pool during TIG welding. Mathematical relationships were also established between input and analysis parameters. This study indicates that the input power is the most significant parameter.

Keywords— TIG, Welding, Temperature, Weld pool

1. INTRODUCTION

TIG welding process is a non consumable arc welding process in which tungsten electrode to produce the weld. The weld zone is shielded from atmosphere with a layer of inert gas [1]. Development of TIG welding process has opened the scope for joining of many materials like stainless steel [2]. Lots of work is done in the area of TIG welding for the optimization of parameters. In this process, the welding parameters are weld speed, current, voltage, input power, gas flow, etc. Figure 1 shows the formation of weld pool during tungsten inert gas welding, tungsten electrode is considered as cathode and workpiece is considered as anode [19].

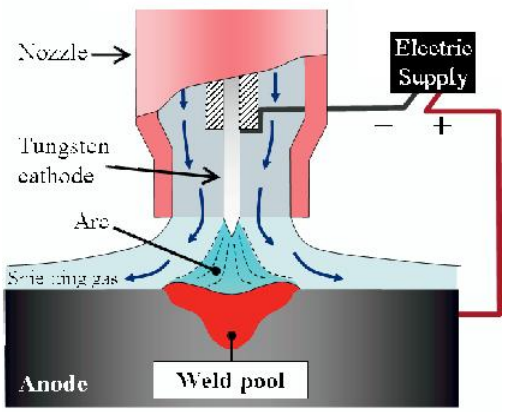

Fig. 1 Formation of weld pool.[19]

Several researchers [3-11] have performed experimental research of tungsten inert gas welding for optimization of process parameters which includes current, weld speed, weld structure, shielding gas, etc for the investigation on the analysis parameters such as mechanical properties, morphology, microstructure, weld bead geometry, etc. These investigations were based on regression analysis and analysis of variance used for prediction of effect of process parameters over the analysis parameters. Scholars [12-17] have also worked on the simulation and finite element analysis for prediction of temperature distribution and residual stresses developed during tungsten inert gas welding (TIG) welding process. Simulation of welding process in one of the emerging area which is beneficial for the researchers and scholars. This method can be adopted for predictions related to the weld pool and temperature distribution which is responsible for heat affected zone and weld bead geometry. Researchers [18-22] have also performed simulations and analysis for prediction of several aspects related to weld pool during TIG welding. They discussed the mechanism and dynamics of weld pool. The weld pool formation is an important aspect which can be considered for simulation based predictions. Further, experiments can be performed on the basis of data generated through simulation. The weld pool geometry or shape includes the length, width, and depth.

2. PRESENT WORK

In the present work, an attempt is made to investigate the temperature distribution and the effects of weld speed (WS) and power input (P) on the weld pool geometry during TIG welding of 304 stainless steel. The shape of weld pool is responsible for the intensity of heat affected zone. The steady state conduction model of fusion or moving heat source is developed by using Smartweld application. The Simulation runs are performed in accordance with taguchi L9 technique. The Regression model has been developed in order to investigate the influence of process parameters.

Smartweld was developed by Sandia National laboratories. It is used for determining the temperature distribution adjacent to a weld when three dimensional heat flow predominates [23].

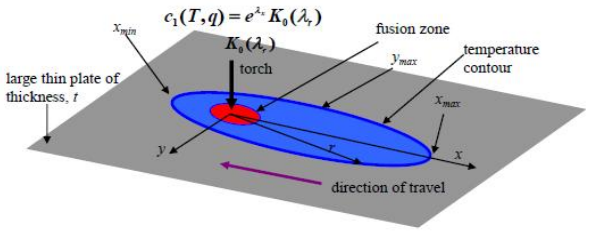

Fig. 2 Conduction Heat flow model.

The steady state model is based on the Rosenthal moving point source (shown in figure 2) to the conduction heat flow equation which is as follows [23]:

$$\frac{2\pi(T-T_0)k_s t}{q} = e^{\left(\frac{vx}{2\alpha_s}\right)} K_o\left(\frac{vr}{2\alpha_s}\right) \qquad (1)$$

where,
T = contour temperature of interest (°C)
To = base metal temperature
k_s = thermal conductivity of metal (J/ms°C)
t = thickness of metal plate (mm)
q = energy (heat) input to the metal (J)
v = welding speed (mm/s)
α_s= thermal diffusivity of metal (m^2/s) [23]

Plates of 304 stainless steel with thickness 10 mm is considered for TIG welding. The welding boundary conditions and range of process parameters are adopted from the previous research work [17].

The range of process parameters is shown in table 1. Three levels of weld speed (WS) and power input (P) were selected which are suitable for tungsten inert gas welding. All other parameters were kept constant. The weld pool geometry (length, width and depth) were observed for all 9 simulation runs (table 2) as per the taguchi design of experiment.

Table 1. Parameters and their level

S.No.	Parameter	Level I	Level II	Level III
1	Weld speed (WS)mm/s	1.5	2.35	3.2
2	Power Input (P) Watts	1200	2887.5	3375

Table 2. The Taguchi L9 design with two factors-each three levels along with their responses.

#Runs	Weld Speed (mm/s)	Input Power (Watts)	Length (mm)	Width (mm)	Depth (mm)
1	1.50	1200	6.03	5.56	2.78
2	1.50	2887.5	12.90	10.50	5.26
3	1.50	3375	14.70	11.70	5.85
4	2.35	1200	5.67	4.96	2.48
5	2.35	2887.5	12.10	9.05	4.52
6	2.35	3375	13.90	10.00	5.00
7	3.20	1200	5.44	4.54	2.27
8	3.20	2887.5	11.70	8.08	4.04
9	3.20	3375	13.40	8.89	4.45

3. RESULTS AND DISCUSSSION

In this section the results of simulation and regression analysis is discussed. The temperature distribution is observed by ISO-3D module of Smartweld application [23]. The regression analysis and analysis of variance was done by using Minitab 17.0.[24]

A. Temperature Distribution

The temperature distribution obtained by simulation is symmetrical throughout the 304 stainless steel plates. Figure 3.1and 3.2 shows the simulated temperature distribution across the plates during the welding process with the weld pool shown in red color and numbered as 1 which represents the molten metal and 2- 5 are the temperature contours adjacent to the weld zone. Weld pool geometry for different temperature contours along with its values are shown in table 3. Graph (figure 4) shows the variation of length, width and depth of weld pool for corresponding temperature at contours 1 to 5 and it is observed that as weld pool (contour1) has minimum dimensions but as we move from contours 2-5, the dimensions increases.

Table 3. Temperature contours and their dimensions

Contour Number	Temperature (ºC)	Length (mm)	Width (mm)	Depth (mm)
1*	**1454**	**6.03**	**5.56**	**2.78**
2	1180	7.25	6.35	3.27
3	910	9.12	7.94	3.97
4	640	12.5	10.3	5.13
5	380	20.1	14.7	7.037

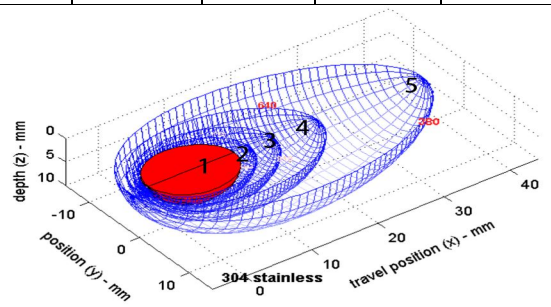

Fig. 3.1 Temperature distribution for Simulation run-1

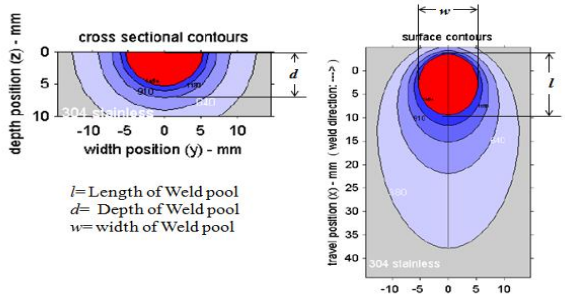

Fig. 3.2 Weld Pool Geometry

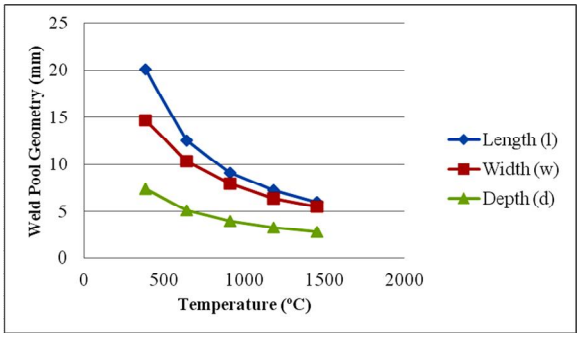

Fig. 4 Variation of weld pool geometry with respect to contour temperatures for Simulation run-1

B. Regression Analysis

In order to analyse the effect of TIG welding parameters on weld pool geometry, main effect and interaction plots were obtained by using multiple regression analysis.

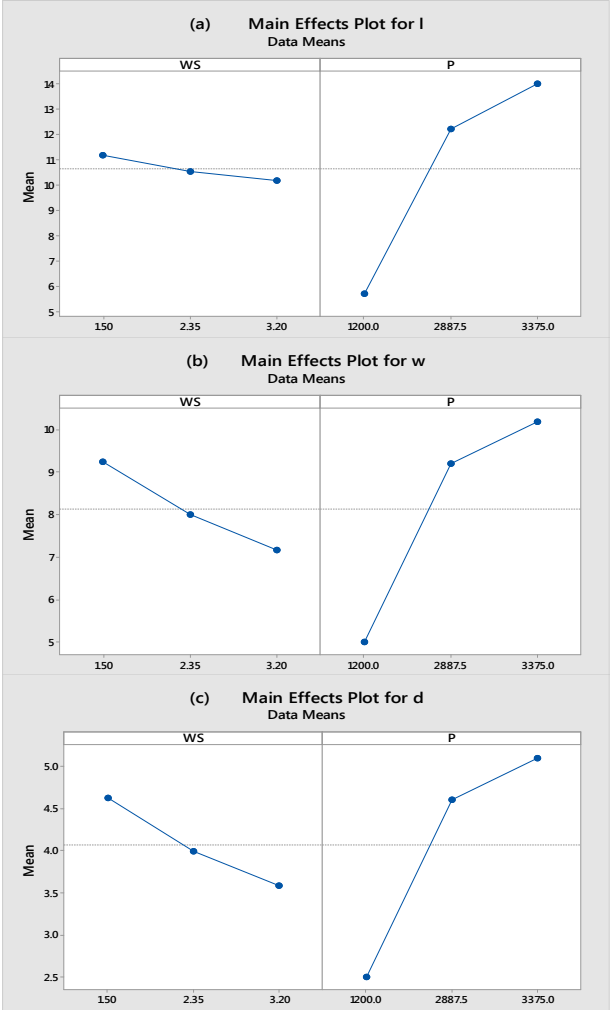

Fig.5 Main effect plots of weld speed (WS) and power input (P) on weld pool geometry (a) Length-*l*, (b) Width-*w* (c) Depth-*d*

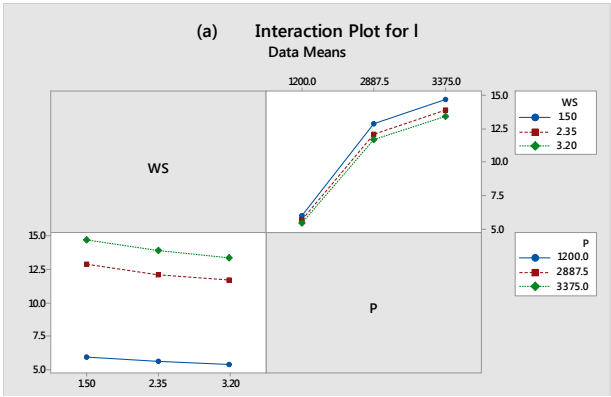

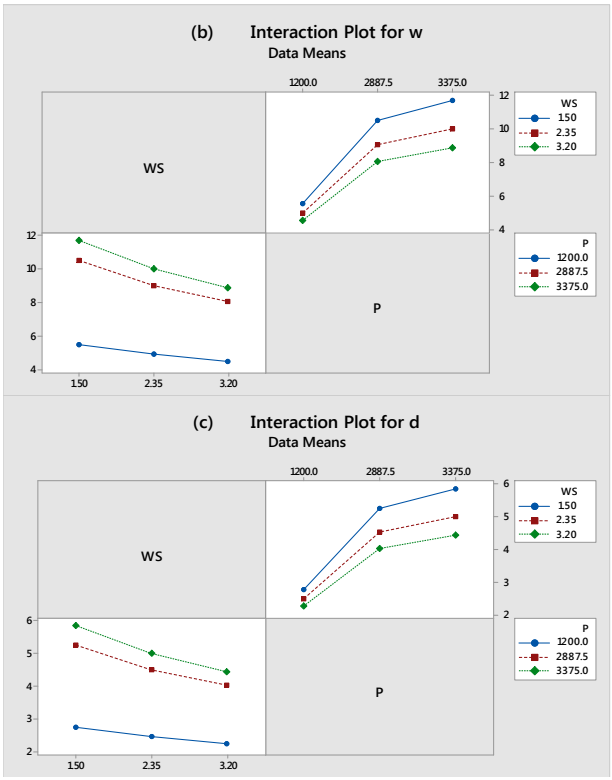

Fig.6 Interaction effect plots for weld speed (WS) and power input (P) on weld pool geometry (a) Length-*l*, (b) Width-*w* (c) Depth-*d*

Figure 5 (a), (b) and (c) shows the main effect plots for weld pool geometry length, width, depth respectively. It is observed that the weld speed has negative influence on weld pool geometry where as power input has positive influence. The variation of weld speed and power input is almost similar for length, width and depth of weld pool. For weld speed from level1 to level2, there is decrease in weld pool geometry but as we move from level 2 to level 3 then the rate decrease is reduced slightly. For power input, there is increase in weld pool geometry from level 1 to2 but the rate of increase is reduced from level 2 to 3.

Figure 6 (a), (b) and (c) shows the interaction plots for weld pool geometry length, width, depth respectively. It is observed that the weld pool geometry is minimum for weld speed of 3.2 mm/s and power input 1200 watts. It is maximum for weld speed of 1.5 mm/s and power input of 3375 watts.

The relationship among weld speed (WS), power input (P) and weld pool geometry i.e. length (l), width (w) and depth (d) during tungsten inert gas welding of 304 stainless steel is obtained through regression analysis by fitting a linear model to analyze the significant process parameter for weld pool geometry, the regression equations formed are as follows:

$$l = 2.561 + 0.003824\,P - 0.6059\,WS \qquad (2)$$

$$w = 5.035 + 0.002407\,P - 1.225\,WS \quad (3)$$

$$d = 2.519 + 0.001204\,P - 0.614\,WS \quad (4)$$

Table 4(a). ANOVA for Length

Source	Sum of Squares	df	Mean Square	F Value	p-value Prob>F	%C
Regression	115.877	2	57.938	1678.42	<0.0001	99.82
P	114.285	1	114.285	3310.75	<0.0001	98.45
WS	1.591	1	1.591	46.10	<0.0001	1.37
Residual	0.207	6	0.035		-	0.18
Cor Total	116.084	8			-	100

Table 4(b). ANOVA for Width

Source	Sum of Squares	df	Mean Square	F Value	p-value Prob>F	%C
Regression	51.783	2	25.8916	149.00	<0.0001	98.03
P	45.273	1	45.2728	260.54	<0.0001	85.70
WS	6.510	1	6.5104	37.47	0.001	12.32
Residual	1.043	6	0.1738		-	1.97
Cor Total	52.826	8			-	100

Table 4(c). ANOVA for Depth

Source	Sum of Squares	df	Mean Square	F Value	p-value Prob>F	%C
Regression	12.965	2	6.48	147.99	<0.0001	98.01
P	11.333	1	11.33	258.71	<0.0001	85.67
WS	1.633	1	1.633	37.27	0.001	12.34
Residual	0.2629	6	0.043		-	1.99
Cor Total	13.23	8			-	100

The ANOVA results for weld pool geometry i.e. Length (l), Width (w) and Depth (d) are shown in Table 4 (a),(b),(c) and (d) respectively. It is found that the selected taguchi model was significant. Power input was the most significant parameter having maximum contribution. Weld speed was other parameter which affected the weld pool length far less than power input.

4. CONCLUSIONS

In case of TIG welding process, suitable weld pool geometry is responsible for successful joining of two 304 stainless steel plates. In order to analyze the effect of process parameters such as weld speed and power input on the weld pool geometry, the simulation of TIG welding was performed through Smartweld application in accordance with Taguchi L9 orthogonal design. The Regression analysis was performed in order to establish mathematical relation among the parameters can be used for prediction of weld pool geometry during TIG welding of 304 stainless steel for the selected range of process parameters. From the analysis of variance, it is observed that power input has 98.45%, 85.70% and 85.67% contribution on length, width and depth respectively. It can be concluded that the most significant parameter is power input which has high percentage of contribution on responses.

REFERENCES

[1] H. B. Cary, Modern Welding Technology, Prentice Hall, Englewood Cliffs, New Jersey, 1989.
[2] Capelli, F. "TIG Welding of Stainless Steel." Tecnol. Mecc. 39.8 (1988).
[3] Indira Rani, M., & Marpu, R. N. Effect of Pulsed Current Tig Welding Parameters on Mechanical Properties of J-Joint Strength of Aa6351. The International Journal of Engineering And Science, 1(1), 1-5, 2012
[4] Hussain, A. K., Lateef, A., Javed, M., & Pramesh, T, Influence of Welding Speed on Tensile Strength of Welded Joint in TIG Welding Process. International Journal of Applied Engineering Research, Dindigul, 1(3), 518-527, 2010
[5] Yuri,T., Ogata, T.,Saito.M.,& Hirayama,Y, Effect of welding structure and δ- ferrite on fatigue properties for TIG welded austenitic stainless steels at cryogenic temperatures. Cryogenics, 40, 251-259, 2000.
[6] Norman, A. F., Drazhner, V., & Prangnell, P. B. Effect of welding parameters on the solidification microstructure of autogenous TIG welds in an Al– Cu–Mg–Mn alloy. Materials Science and Engineering: A, 259(1), 53-64.
[7] Wang, Q., Sun, D. L., Na, Y., Zhou, Y., Han, X. L., & Wang, J. (2011). Effects of TIG Welding Parameters on Morphology and Mechanical Properties of Welded Joint of Ni-base Superalloy. Procedia Engineering, 10, 37-41.
[8] Kumar, A., & Sundarrajan, S. (2009). Optimization of pulsed TIG welding process parameters on mechanical properties of AA 5456 Aluminum alloy weldments. Materials & Design, 30(4), 1288-1297.
[9] Durgutlu, A. (2004). Experimental investigation of the effect of hydrogen in argon as a shielding gas on TIG welding of austenitic stainless steel. Materials & design, 25(1), 19-23.
[10] Li, D., Lu, S., Dong, W., Li, D., & Li, Y. (2012). Study of the law between the weld pool shape variations with the welding parameters under two TIG processes. Journal of Materials Processing Technology, 212(1), 128-136.
[11] Lothongkum, G., Viyanit, E., & Bhandhubanyong, P. (2001). Study on the effects of pulsed TIG welding parameters on delta-ferrite content, shape factor and bead quality in orbital welding of AISI 316L stainless steel plate. Journal of Materials Processing Technology, 110(2), 233-238.
[12] Tseng, K. H., & Hsu, C. Y. (2011). Performance of activated TIG process in austenitic stainless steel welds. Journal of Materials Processing Technology, 211(3), 503-512.
[13] Narang, H. K., Singh, U. P., Mahapatra, M. M., & Jha, P. K. (2011). Prediction of the weld pool geometry of TIG arc welding by using fuzzy logic controller. International Journal of Engineering, Science and Technology, 3(9), 77-85.
[14] Karunakaran, N. (2012). Effect of Pulsed Current on Temperature Distribution, Weld Bead Profiles and Characteristics of GTA Welded Stainless Steel Joints. International Journal of Engineering and Technology, 2(12).
[15] Raveendra, A., & Kumar, B. R.(2013). Experimental study on Pulsed and Non- Pulsed Current TIG Welding of Stainless Steel sheet (SS304). International Journal of Innovative Research in Science, Engineering and Technology, 2(6)
[16] Preston, R. V., Shercliff, H. R., Withers, P. J., & Smith, S. (2004). Physically based constitutive modelling of residual stress development in welding of aluminium alloy 2024. Acta Materialia, 52(17), 4973-4983.
[17] Akbari Mousavi, S. A. A., & Miresmaeili, R. (2008). Experimental and numerical analyses of residual stress distributions in TIG welding process for 304L stainless steel. journal of materials processing technology, 208(1), 383-394.
[18] Hong Wang, XiangZhang, XingChen, Zhiwei Liu, The Weld Pool Dynamics In The Tandem Welding, International Journal of Research in Engineering and Technology, Vol.04 Issue: 12, Dec-2015
[19] M. Ito, S. Izawa, Y. Fukunishi, and M. Shigeta, SPH Simulation of Gas Arc Welding Process, Seventh International Conference on Computational Fluid Dynamics (ICCFD7), Big Island, Hawaii, July 9-13, 2012
[20] H. K. Narang, U. P. Singh, M. M. Mahapatra and P. K. Jha, Prediction of the weld pool geometry of TIG arc welding by using fuzzy logic controller, International Journal of Engineering, Science and Technology Vol. 3, No. 9, 2011, pp. 77-85.

[21] A. H. Faraji, A. Bahmani, M. Goodarzi, S. H. Seyedein, M. O. Shabani, Numerical and experimental investigations of weld pool geometry in GTA welding of pure aluminum, **J.** Cent. South Univ. (2014) 21: 20−26,
[22] Zeniya Tasuku, Tashiro Shinichi , Tanaka Manabu, Yamamoto Eri, Yamazaki Kei and Suzuki Keiichi, Numerical analysis of weld pool formation mechanism in TIG welding in consideration of the influence of emitter material adding to the tungsten cathode, Transactions of JWRI, Vol.39 (2010), No. 2.
[23] G. Richard Eider and Phillip W. Fuerschbach, Smartweld Optimization and Analysis Routines An Extensible Suite of Codes for Weld Analysis and Optimal Weld Schedules, Sandia Report, SAND96-2378 UC-1420, National Technical Information Service, US Department of Commerce, Nov 1996.
[24] Shonda & Jeffrey Sklar, Minitab Manual, Pearson Education, Inc., 2013